Two Cross-Equatorial Sections at 110°W

ANTS LEETMAA AND ROBERT L. MOLINARI

National Oceanic and Atmospheric Administration, Atlantic Oceanographic and Meteorological Laboratory, Miami, FL 33149

(Manuscript received 26 May 1983, in final form 22 September 1983)

ABSTRACT

A section along 110°W in the eastern Pacific from about 6°N to 6°S was occupied in March and June of 1981. Measurements consisted of absolute velocity profiles and CTD casts. The large-scale structure of the subsurface zonal flow remained relatively invariant between these cruises. The Equatorial Undercurrent and North and South Equatorial Undercurrents appear as strong eastward flows, separated by westward currents. Away from the equator, comparison of currents estimated geostrophically with the direct observations indicate that the two techniques are in agreement within estimated errors except close to the surface. In the vicinity of the equator the geostrophic technique in general fails and the directly measured currents must be used. During March, within 3° of the equator from the surface to 700 m, the flow was more eastward by about 0.15 m s^{-1} than in June. In March, the flow and temperature fields were relatively symmetric about the equator. By June, strong asymmetries had developed. In the top 100 m, eastward flow extended from the Undercurrent to about 3°S. A strong, shallow westward flow was situated over and to the north of the Undercurrent. A shallow southward flow developed from 4°N to 2°S. Order-of-magnitude estimates suggest that this can advect westward momentum onto the equator in the top 50 m and modify the Undercurrent. Asymmetry also developed in the near-surface thermal field. In June, upwelling was primarily located south of the equator. This resulted in a cold band lying south of the equator at the core of which the flow was predominantly eastward. A strong meridional temperature gradient at the equator separated the colder water from warmer water to the north. These asymmetries develop presumably in response to the seasonal increase from March to June of the winds. Computations of zonal transports in various σ_t-classes in the near-surface layers suggest that the bulk of the Undercurrent water does not return west on the same density surfaces, but does so in the surface layers.

1. Introduction

Most of what is known of equatorial and near-equatorial current distributions in the eastern Pacific Ocean has been inferred from some combination of geostrophic computations, sea-level variations and property distributions (Hayes *et al.*, 1983; Wyrtki, 1974; Tsuchiya, 1981, for instance). The major currents observed in the eastern central Pacific are thought to be primarily zonal. The flow field is complex: Tsuchiya (1975), among others, has shown that up to four distinct eastward countercurrents exist on both sides of the equator. He refers to the surface flows as the South and North Equatorial Countercurrents (SECC and NECC) and suggests that the flows with subsurface velocity cores be referred to as the South and North Equatorial Undercurrents (SEUC and NEUC). We will follow the same nomenclature. The core of the Equatorial Undercurrent (EUC) lies close to the equator. The flow directly above the EUC can be either to the east or west. The South Equatorial Current (SEC) flows to the west both south and north of the equator in the surface layers. Leetmaa (1982) points to the existence of an eastward flow separate from the EUC, located just south of the equator. This appears seasonally, and divides the SEC into two parts.

Equatorial Pacific Ocean Climate Studies (EPOCS) is a NOAA program for the study of the origin of anomalous sea-surface temperatures (SST) and their effect on global climate. As part of EPOCS, cruises were made to the eastern Pacific Ocean to observe current distributions along 110°W and to study their possible role in SST evolution. Absolute velocity-profiler [Pegasus (Spain, Dorson, and Rossby, 1981)] stations were occupied from approximately 7°S to 6.5°N during March and June 1981 aboard the NOAA Ship *Oceanographer*. Details of Pegasus performance are given by Spain *et al.* (1981) and Leetmaa (1982). On the average, Pegasus speed measurements are accurate to better than 0.05 m s^{-1}. However, close to the surface, errors can be larger than this. High-frequency motions such as tides or low-frequency variability can have equivalent or higher amplitudes. EPOCS mooring measurements at 110°W and 0° indicate that the semidiurnal tide has an amplitude of about 0.1 m s^{-1}. The same data indicate that lower-frequency motions such as the 20 and 30 day waves have amplitudes of 0.1–0.3 m s^{-1}. Hence the instrumental noise is generally

less than possible aliasing by time-dependent motions. A Neil Brown Instrument System (NBIS) Mark III CTD/O_2 system was used to obtain CTD data. Data acquisition and processing techniques are discussed by Mangum *et al.* (1980).

These velocity sections provide a description of the absolute velocity field along 110°W in the equatorial eastern Pacific Ocean during two phases of the annual cycle. Typically in March, near equatorial sea-surface temperatures (SST) reach their maximum values and eastward flow is frequently found at the surface close to the equator. Usually by June this is replaced by westward flow and lower temperatures appear south of the equator. This was also the case in 1981. These results are compared to previous descriptions of the current field deduced from indirect techniques. Off the equator, geostrophic computations appear to be adequate to define the deeper velocity field. Hayes (1982) has shown that at times the geostrophic approximation also works on and close to the equator. This apparently was not the case during June 1981.

2. Observations

a. Zonal velocity sections

Vertical sections of the absolute zonal velocity are shown in Fig. 1 for March and June 1981. The large-scale pattern of flow in March was relatively symmetric about the equator. The speed core of the EUC lay just south of the equator. Peak speeds were over 1.3 m s^{-1}. Eastward flow also extended to the sea surface. Moored current meter observations at this location from 1980 to 1982 indicated that eastward surface flow occurs during February–April of each year (Halpern, personal communication, 1983). Historical ship drift observations (Puls, 1895) show eastward flow from ~120° to 90°W in March and April. The surface flow north and south of 0° was predominately to the west. Velocities approaching 1.0 m s^{-1} were found from 2.5° to 3.0°N. They were 0.6 m s^{-1} at 4.5°S. The strongest westward flow was confined above 100 m. North of 4°N the flow was to the east. Above ~50 m, this is the NECC. There was no comparable eastward surface flow south of the equator at similar latitudes. Below 100 m, the NEUC and SEUC were symmetrically located about the equator at about 5°N and 5°S. The NEUC had core speeds of about 0.6 m s^{-1}. The SEUC was weaker with core speeds of about 0.2 m s^{-1}. Eastward flow of 0.1–0.2 m s^{-1} extended to at least 700 m over large areas between about 3°S and 2°N. Two regions of westward flow, confined to within a degree of the equator, were situated at ~300 and 600 m.

In June, poleward of about 3° the pattern looked similar to that observed in March, although the magnitudes of the major currents had changed. Within 3° of the equator, the flow pattern was more asymmetric. Eastward flow in the top 100 m extended from 1° to 3°S. North of 1°S, the near-surface flows were westward; speeds greater than 1.0 m s^{-1} were measured just north of the equator. This asymmetry extended below the Undercurrent. Flow south of the equator tended to be eastward while westward flow lay to the north. The bulk of the flow beneath the EUC was westward. Two regions with higher speeds were situated at about 300 and 500–600 m. These were also observed in March. The speed axis of the EUC was again located just south of 0°. In and below the core of the EUC, zonal speeds were ~0.1–0.15 m s^{-1} less than in March.

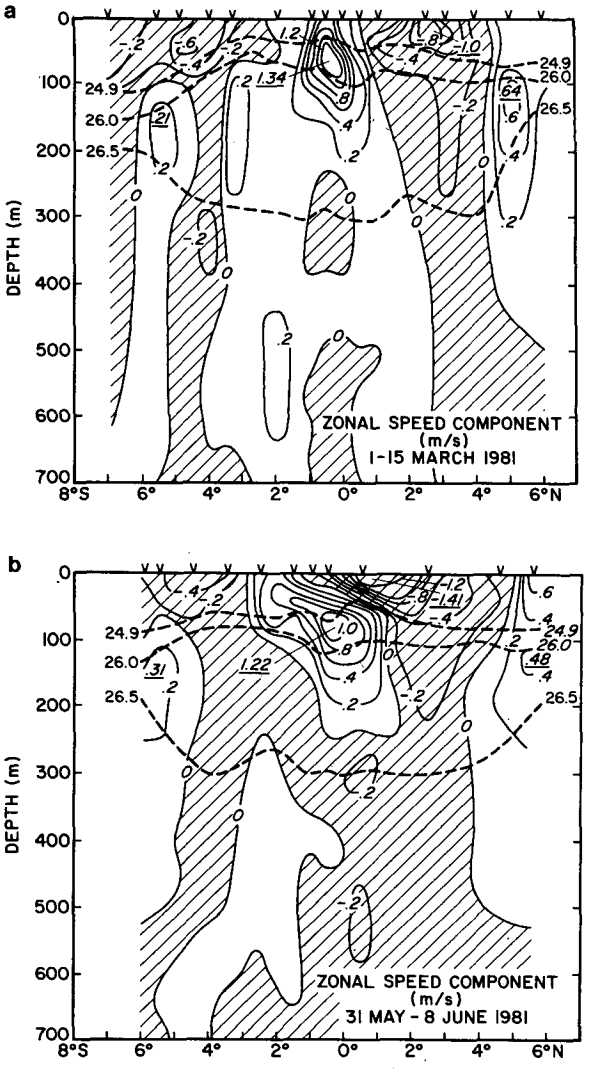

FIG. 1. Zonal velocity sections along 110°W for (a) 1–15 March 1981 and (b) 31 May–8 June 1981.

b. Meridional velocity field

The meridional velocities for the two cruises are shown in Fig. 2. Regions of prominent meridional flow were associated with the major currents. The northward flow between 4° and 6°S during March was

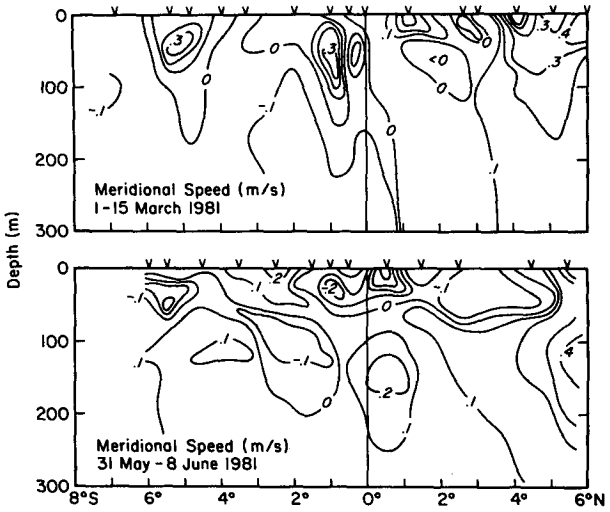

FIG. 2. Meridional velocity section along 110°W (upper panel) 1–15 March 1981 and (lower panel) 31 May–8 June 1981.

associated with the westward maximum in the SEC. The northward flow north of 4°N was in the area of the NECC and NEUC. At the core of the NEUC this component was 0.25 m s^{-1} in March and over 0.4 m s^{-1} in June. The meridional component in the SEUC in June was about 0.1 m s^{-1}.

A convergent region was present during March in the vicinity of the core of the EUC. This was not observed in June. In the top 50 m, the flow in June was to the south from ~4°N to 2°S. There is an indication of a convergence near the surface at 0°, coincident with a thermal front (Fig. 3b). A similar southward flow was also observed farther to the east in June 1981 and December 1982 (Leetmaa and Wilson, 1983). Subsurface southward flow extends across the equator to about 2°S where there is a suggestion of a convergence between ~20 and 60 m. Possibly there is upwelling into the surface layers where the velocities are not well defined by the Pegasus measurements. This is suggested in the thermal field (Fig. 3b). The coincidence of the southward flow and the extension of eastward flow south of the EUC above the thermocline suggests that the near-equatorial meridional circulation might play an important role in the dynamics of the upper layers of the EUC. This possibility is further explored in the discussion.

c. *Temperature sections*

The temperature sections taken along 110°W during March and June are shown in Fig. 3. Seasonally, highest surface temperatures in this region occur during March through May. At this time an equatorial minimum of 1–2°C can still exist. Robinson (1976) shows a patch of lower equatorial SSTs extending from ~110° to 130°W during March and April. However, the 3.5°C difference between equatorial temperatures and those poleward of 2° during March 1981 is larger than the climatological difference. Examination of continuous temperature records at 15 m from a mooring at the equator (Halpern, personal communication, 1983) shows a short-term cooling event occurring in early March. Temperatures dropped from about 22°C in February to 18.5°C in early March and then rose again. By late March, temperatures were over 25°C. Presumably, such events contribute to the maintenance of the cold water patch as shown on climatological atlases.

The thermocline was uplifted between 4°N and 4°S in March. Between 3°N and 3°S, the surface dynamic height relative to 500 m was ~0.06 dyn-m less than in June or than the average for all the past EPOCS cruises (Hayes *et al.*, 1983). A westward surface flow of about 0.8 m s^{-1} centered around 3°N (Fig. 1) was

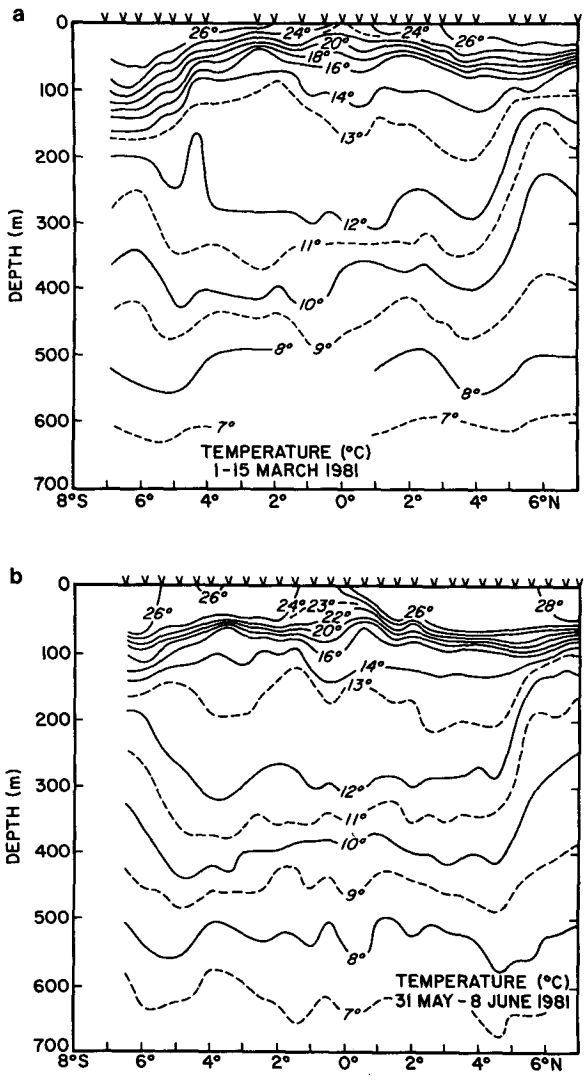

FIG. 3. Temperature sections along 110°W for (a) 1–15 March 1981 and (b) 31 May–8 June 1981.

associated with the meridional dynamic height gradient at the edge of the uplifting. South of the equator the maximum westward flow was weaker at 0.6 m s^{-1} and was located south of the maximum dynamic height gradient. Possibly the station spacing did not resolve the core of the westward flow. Both north and south of the equator this westward flow extends into the deep water. The occurrence of the shallower-than-average thermocline with strong eastward flow in the vicinity of the equator at first sight is surprising. If the eastward flow was quasi-geostrophically balanced, one might have expected a deepening of the thermocline and an increase in the dynamic height in the vicinity of the equator. The eastward flow in March was about 0.15 m s^{-1} greater than in June. At 1° a dynamic height gradient of 0.006 dyn-m over one degree would be needed to balance this. A relative increase in gradient in the vicinity of the equator of this magnitude was observed. The large-scale symmetric structure apparent in the March velocity and temperature section is suggestive of the first meridional, gravest-vertical-mode baroclinic Rossby wave. This wave would exhibit the enhanced westward flow off the equator and eastward flow in the vicinity of the equator as seen in March (Fig. 1). Sea-level measurements from the Galápagos Islands indicate a drop in sea level there in late January (Hayes and Halpern, 1983). If this were the signature of an upwelling Kelvin wave, the reflected Rossby wave from the eastern boundary would arrive back at 110°W in early March. Hence, there is some corroborative evidence to support our suggestion.

A large region exists below the thermocline where the vertical temperature gradient is relatively small. This is most pronounced between the 12 and 13°C isotherms. This feature has become known as the thermostad and appears to be a quasi-permanent feature in the central and eastern Pacific (Stroup, 1969). The NEUC and SEUC lie at the northern and southern extremes of the thermostad. The position of the NEUC relative to the thermostad was extensively discussed by Hayes *et al.* (1983).

In the June section SSTs north of 3°N increased by 1–2°C from March, whereas south of the equator they were 0.5 to 1°C lower. Hence, the near-surface temperature field became asymmetric about the equator. A strong horizontal temperature gradient of about 2°C over 50 km was situated at the equator. The strong westward flow (Fig. 1) lay just to the north of this. Cooler surface waters and possible upwelling appear between about 2°S and 0°. Upwelled water comes from the top of the thermocline at about 50 m. The spreading apart of the isotherms just south of the equator occurs in the vicinity of the core of the EUC. There is a strong uplifting of isotherms warmer than 15°C just north of 0° which modifies this spreading. The uplifting is related to the strong westward shear at this location between the core of the EUC and the surface velocities (Fig. 1). It is not clear what balances the northward shoaling of the isotherms south of the equator.

d. Salinity distribution

The salinity sections for March and June 1981 are shown in Fig. 4. The main features during both sections were similar. The salinity distribution above about 400 m was asymmetric about the equator. Saltier water lies south of the equator; fresher water to the north. Highest salinities were found in the thermocline at 6–7°S. A band of this higher-salinity water extended northward in and above the thermocline to about 0°30′S. The subsurface maximum of 35.2–35.4‰ just south of the equator is carried eastward by the EUC (Tsuchiya 1968). This maximum lies at a density of σ_t-value of 25.0. The southern maximum lies at a den-

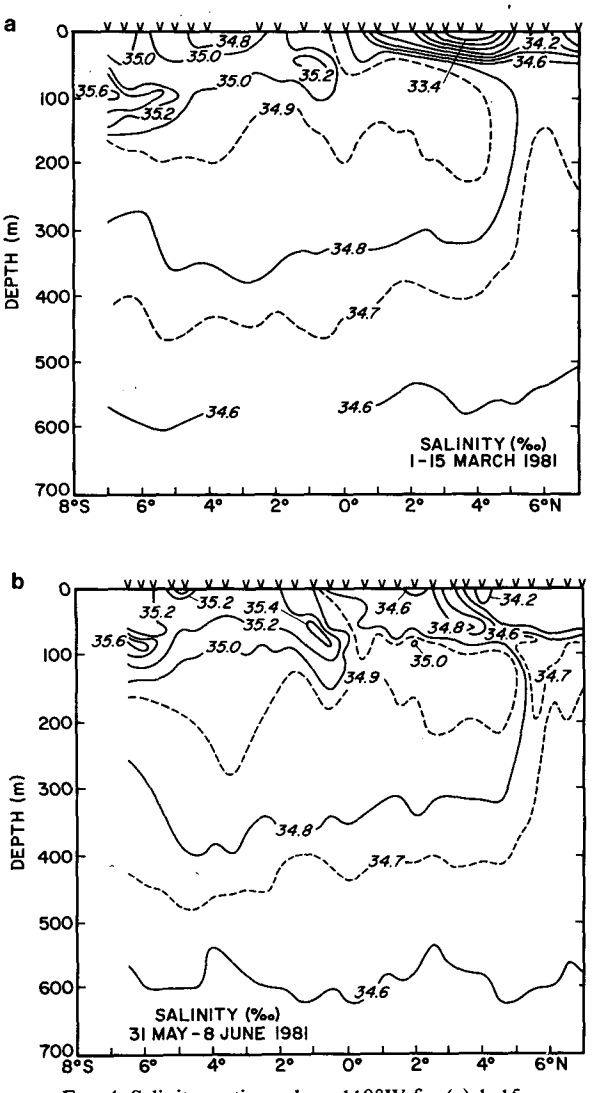

FIG. 4. Salinity sections along 110°W for (a) 1–15 March 1981 and (b) 31 May–8 June 1981.

sity of about 24.5 and originates in the subtropics south of the equator. Presumably it is carried westward in the SEC (Tsuchiya, 1968). In the region between these maxima the salinities in the thermocline were greater than 35‰.

South of the equator during March the SEC was stronger than in June. In the mixed layer it appears to carry fresher water westward from the vicinity of the eastern boundary. In March, salinities less than 34.8‰ were associated with the core of the SEC. In June when the SEC was weaker, salinities for the most part were over 35.0‰.

The low salinities north of the equator presumably are related to the high precipitation in the ITCZ which lies closest to the equator during northern spring. In March salinities were as low as 33.4‰. The southern position of the ITCZ and westward advection of low-salinity water from east of the Galápagos probably were major contributors to these low values.

Below the thermocline, a region of salinity greater than 34.9‰ extends northward across the equator. In both sections this contains small regions with values greater than 35.0‰ at about 100 m at 2°N. These higher salinities perhaps indicate recirculation of EUC water to the west.

e. Surface temperature distributions

Surface temperature values along the cruise track between 85 and 110°W in June are shown in Fig. 5. Lowest temperatures were found in a narrow band between 1°S and 2°S from 85 to 110°W. Lowest temperatures in this band were found near the Galápagos Islands. The near-surface flow at 110°W in the vicinity of the cold band was eastward. This is clearly shown in Fig. 6. The coincidence of lowest temperature and eastward flow was also observed in March although the mechanisms were different. Westward advection of cold water from the Galápagos or the coastal regions does not seem to be a direct factor in producing this cold tongue. It is produced locally by upwelling south of the equator that is caused by the meridional and zonal components of the wind stress (Cromwell, 1953; Leetmaa and Wilson, 1983).

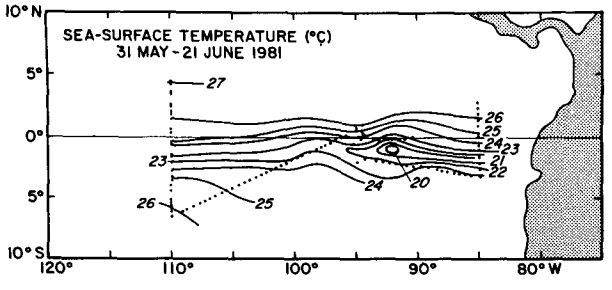

FIG. 5. Surface temperature values determined from XBTs and bucket temperatures alongruise track, 31 May–21 June 1981.

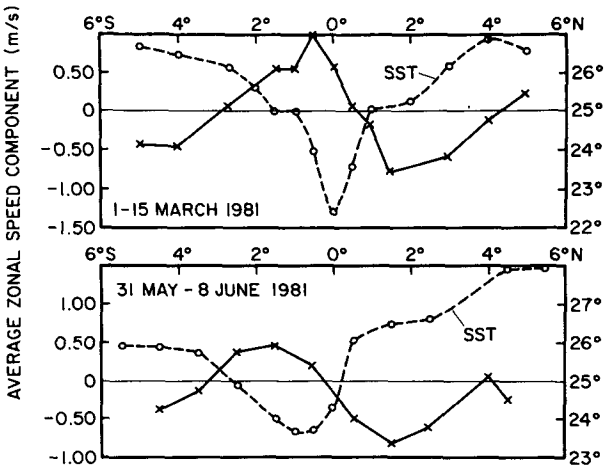

FIG. 6. Zonal surface velocities from Pegasus casts compared to meridional sea surface temperature distribution at 110°W for the time periods shown.

f. Intercomparisons between geostrophic and Pegasus profiles

Differences between Pegasus and geostrophic zonal speed components are plotted in Fig. 7. In general, after accounting for the speed at the geostrophic reference level, the difference curves show that below 100 m the major currents are strongly geostrophic. Those curves that do have systematic differences at depth, March at 5.5°S (not shown), March at 4°S and 3°N and June at 4.5°S, occur on or near boundaries between eastward and westward flows at these depths (Fig. 1). The different horizontal interval sampled by the Pegasus (point measurement) and geostrophic (typically an average over 110 km) observations could account for this lack of agreement.

Systematic differences between the Pegasus and geostrophic profiles do occur above 100 m (Fig. 7). Ekman transports have been computed by assuming constant winds for the following intervals: March, 4°–6°N (u = 2.5 m s^{-1}, v = −2.5 m s^{-1}), 7°S–3°N (2.5 m s^{-1}, 2.5 m s^{-1}); and June, 4°–6°N (−5 m s^{-1}, 5 m s^{-1}), 7°S–3°N (5 m s^{-1}, 5 m s^{-1}). These were the values observed on the cruises. Average Ekman layer speeds have been computed assuming that the Ekman layer is 60 m thick and are plotted in Fig. 6 relative to the reference level speed. Except at 2.5°S during June, the surface flow is in the same direction as predicted by the Ekman theory; however, the magnitude of the observed differences are typically greater than predicted by the simple quadratic law theory. Several factors can contribute to these discrepancies: inability of the Pegasus to adequately resolve near-surface flows, geostrophic flows with spatial scales less than the 110 km station spacing, direct wind-driven surface flows and other ageostrophic flow components. The data are inadequate to resolve which factors were most important.

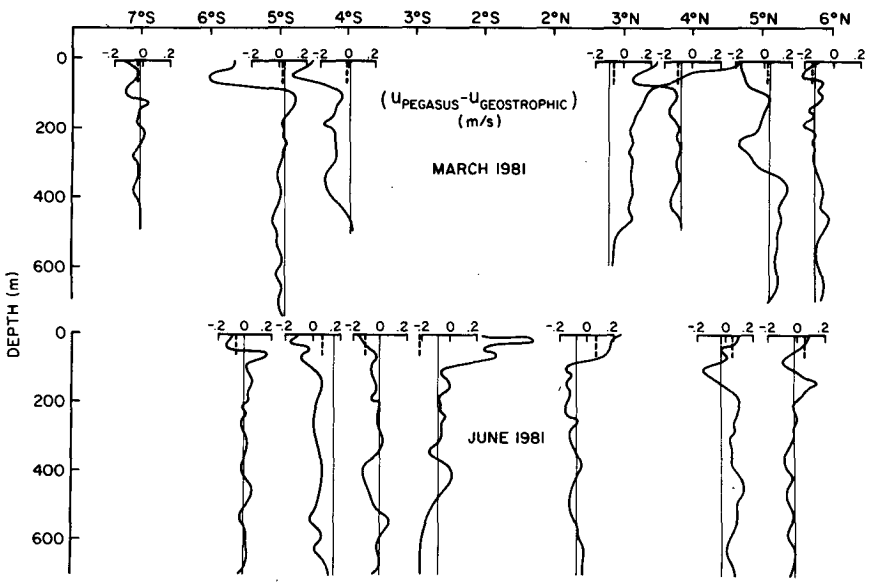

FIG. 7. The differences between Pegasus zonal velocities and geostrophic estimates. The latter were shifted to coincide with the directly observed velocities at 1000 m.

All that can be concluded is that Ekman flows may account for some of the ageostrophic component of flow observed at the surface.

3. Discussion

There is a seasonal fluctuation in the strength and direction of the wind forcing in the eastern Pacific. In the northern spring the ITCZ moves closer to the equator and both the meridional and zonal components of the stress decrease in amplitude. Direct wind measurements from the mooring at 110°W and 0° during 1980–81 showed that the daily averaged winds reached a maximum in November 1980 of over 5 m s^{-1} to the west and 4 m s^{-1} to the north. In March 1981 the zonal component dropped to zero and the meridional component decreased to about 2.5 m s^{-1}. By June 1981 the westward and northward components were again about 5 m s^{-1}. These changes in addition to changes in remote winds caused a strong asymmetry to develop in the near-surface current and temperature structure. By June a band of low temperatures appeared south of the equator at 1–2°S that extended eastward to 85°W. Strong, shallow westward flow developed on and north of the equator. Eastward flow extended southward from the EUC to ~3°S above the thermocline. A strong, southward cross-equatorial flow developed.

Part of these changes was no doubt caused by the intensification of the meridional winds. However, the zonal stress also intensified and its distribution is also asymmetric about the equator. To assess the role of the meridional winds, the patterns at 110°W during June can be compared to observations farther east at 85°W where the winds are predominately meridional. At 85°W upwelling is strongest between 1° and 2°S (Fig. 5; Leetmaa and Wilson, 1983). Shallow westward flow of 0.10–0.60 m s^{-1} occurs north of the equator. This is weaker than that found at 110°W and presumably the zonal component of the stress at 110°W is required to make it stronger. Cross-equatorial southward flow occurs at the base of the mixed layer and in the main thermocline as at 110°W. A large difference between 110° and 85°W is the absence of a persistent EUC and the shallow eastward flow to the south of it. Eastward flow in the vicinity of the equator at 85°W occurs either seasonally in the spring or during El Niño events (Lucas, 1982). During March 1982 we observed an undercurrent at 85°W and this also was broadened to the south in a region of weak southward flow. In the upwelling zone just south of the equator at 85°W, the near-surface flow is to the west at 0.4 m s^{-1} or greater. Hence, it seems unlikely that the shallow eastward flow south of the equator at 110°W is solely caused by the meridional winds. Southward advection of eastward momentum out of the EUC no doubt contributes to it, but not as the sole source.

The southeast trades around 110°W have a maximum south of the equator. This wind distribution produces a divergence in the directly wind-driven currents that extends farther south than that produced by purely meridional winds. The magnitude of this upwelling is difficult to estimate because the stress distribution is not well known because of infrequent ship traffic in the region. Using the mean winds of Wyrtki and Meyers (1976), Leetmaa (1982) constructed Sverdrup (1947) transport streamlines for this region. Eastward transport was indicated south of the equator. Using the

Wyrtki and Meyers (1976) monthly mean winds in a linear numerical model, Busalacchi and O'Brien (1980) found eastward flow south of the equator in this region from May through December. This results in the model (and in the observations) from an uplifting of the thermocline at about 4°S. Hence upwelling that is produced by the southeast trades has a maximum around 4°S. This upwelling probably is one reason why higher-salinity water was found in the surface layers from 2°S to 6°S in June (Fig. 4b).

The dynamics of the shallow westward flow just north of the equator are probably complex. Except in the top 20 m the westward shear above the Undercurrent within a degree of the equator is not supported by the pressure gradients. Westward momentum is put in at the sea surface by the wind stress. Both components of the stress produce a convergence north of the equator. Nonlinear effects probably are important here as well as in the region of southward flow. The importance of the meridional circulation in the upper part of the EUC is suggested by the magnitude of the term, $v\partial u/\partial y$. The average southward velocity between $\sim$10 and 50 m close to the equator is about 0.1 m s^{-1}. The north–south variation in the zonal flow in this region is about 0.6 m s^{-1} over one degree. Hence the magnitude of $v\partial u/\partial y$ is 5.5×10^{-7} m s^{-2}. This can be compared to the magnitude of the east–west pressure gradient that drives the Undercurrent. This at the sea surface is 4–5 $\times$ 10^{-7} N kg^{-1} (Leetmaa and Spain, 1981). Hence southward advection of westward momentum can be as important as the zonal pressure gradient in the local momentum balance.

From 110°W to the Galápagos, the Undercurrent loses its transport primarily from the upper layers (Stroup, 1969; Taft and Jones, 1973; Leetmaa, 1982). It seems likely that the meridional overturning caused by southerly winds is partially responsible for this. Suppose that the term $u\partial u/\partial x$ is balanced by $v\partial u/\partial y$ whose magnitude was estimated to be 5.5×10^{-7} m s^{-2}. Then $u\Delta u/\Delta x \approx -5.5 \times 10^{-7}$ m s^{-2} where u is the average velocity from 110°W to 95°W and Δx = 15° or 1.6×10^6 m. Hence Δu is -1.8 m s^{-1}. This obviously is too large but it is of the right order of magnitude. Other terms such as the zonal pressure gradient and upwelling caused by the zonal winds must also be important. Careful modeling is required to evaluate the importance of all of these terms.

Several properties of the three subsurface eastward currents are summarized in Table 1. As shown in Fig. 6, the SEUC and NEUC are essentially in geostrophic balance. Included are average properties estimated from geostrophic computations by Tsuchiya (1975) and Hayes *et al.* (1983) to demonstrate the representativeness of the March and June estimates. Within the accuracies of the two different observational techniques, the geostrophic and absolute estimates are similar. The core speeds of the SEUC range from 0.2 to 0.3 m s^{-1} and those of the NEUC from 0.3 to 0.6 m s^{-1}. As observed by Tsuchiya (1975), the core of the SEUC is typically deeper than the core of the EUC. For these four crossings, the average core speed of the EUC was 1.25 m s^{-1} which occurred at an average depth of 75 m.

Transports computed for the three eastward flows are given in Table 2. Also listed are average geostrophic transports computed from several crossings of the NEUC and SEUC as given by Tsuchiya (1975) and Hayes *et al.* (1983). As expected, no systematic differences between the Pegasus and geostrophic transports are discernible. The transport of the shallow eastward flow south of the equator during June was about 7.0×10^6 m^3 s^{-1}.

Transports have also been computed by σ_t-intervals. The intervals were chosen, somewhat arbitrarily, to represent the surface layer (from 0 m to σ_t = 24.9), the core layer of the EUC (σ_t = 24.9 to σ_t = 26.0) and the core layer of the NEUC and SEUC (σ_t = 24.9 to σ_t = 26.5). Their depth distribution is shown in Fig.

TABLE 1. Core properties of the Pacific subsurface eastward currents determined from Pegasus observations along 110°W. Average properties and standard deviations computed from the geostrophic determinations relative to 500 db of Tsuchiya (1975), between 105° and 112°W, and Hayes *et al.* (1983), at 110°W, are also given.

	Current	Maximum zonal speed (m s^{-1})	Depth (m)	Latitude	Surface flow direction
SEUC:	March 1981	0.21	160	5.5°S	Westward
	June 1981	0.31	150	5.5°S	Westward
	Tsuchiya (1975)	0.19 (±0.03)	142 (±13)	—	—
EUC:	August 1980	1.25	90	0°	Westward
	September 1980	1.19	70	0.5°S	Westward
	March 1981	1.34	60	0.5°S	Eastward
	June 1981	1.22	80	0.5°S	Westward
NEUC:	August 1980	0.52	100	5.5°N	Westward
	March 1981	0.64	100	5.0°N	Eastward
	June 1981	0.48	140	5.5°N	Eastward
	Hayes *et al.* (1973)	0.38 (±0.06)	118 (±29)	4.6°N (±0.3)	—
	Tsuchiya (1975)	0.25 (±0.12)	109 (±33)	—	—

TABLE 2. Transports of the eastward equatorial currents in the Pacific Ocean determined from Pegasus and geostrophic observations. The combined transport of the NECC and NEUC is given because of the difficulty in separating the two. Station positions relative to the flow field are shown in Figs. 2–4. Asterisks indicate that the lateral boundaries of a flow have not been crossed.

	Current	Station positions	Transport ($\times 10^6$ m^3 s^{-1})	Remarks
SEUC:	March 1981	5°S, 5.5°S	4.6	Transport within 0-m s^{-1} isotach
	June 1981	4.5°S, 5.5°S, 6°S	9.9*	Transport within 0-m s^{-1} isotach
	Tsuchiya (1975)	—	5.9	Average geostrophic transport relative to 500 db at 105° and 112°W
EUC:	August 1980	0.5°S, 0°, 0.5°N	19.8*	Transport within 0.2-m s^{-1} isotach
	September 1980	1°S, 0.5°S, 0°, 0.5°N	14.2*	Transport within 0.2-m s^{-1} isotach
	March 1981	1°S, 0.5°S, 0°, 0.5°N	23.9	Transport within 0.2-m s^{-1} isotach
	June 1981	0.5°S, 0.5°N	20.3*	Transport within 0.2-m s^{-1} isotach
		2.5°S, 1.5°S, 0.5°S, 0.4°S	27.6	Transport within 0.2-m s^{-1} isotach
NECC/ NEUC:	August 1980	3.5°N, 4.5°N, 5.5°N	14.4*	Transport within 0-m s^{-1} isotach
	March 1981	5°N, 6°N	19.9*	Transport within 0-m s^{-1} isotach
	June 1981	4.5°N, 5.5°N	15.7*	Transport within 0-m s^{-1} isotach
	Hayes *et al.* (1983)	—	22.1	Average geostrophic transport relative to 500 db

1. During both March and June there are transport imbalances in all three layers (Table 3).

From the surface down to the $\sigma_t = 26.5$ surface the net section transports are not zero nor do they need to be. In March above this surface the net transport is about 8×10^6 m^3 s^{-1} to the east. If the deeper water were included, this would still be the case. As pointed out earlier, the main difference between the June and March sections lies within about 3° of the equator. In this region during March the flow is about 0.15 m s^{-1} more to the east than in June. This March increase in eastward flow has been interpreted as a first mode in the vertical Kelvin wave (Hayes and Halpern, 1983).

TABLE 3. Transport ($\times 10^6$ m^3 s^{-1}) by σ_t-interval. Three intervals are given: surface layer (0 m to $\sigma_t = 24.9$), core layer of the EUC ($\sigma_t = 24.9$ to $\sigma_t = 26.0$) and core layer of the NEUC/SEUC ($\sigma_t = 24.9$ to $\sigma_t = 26.5$). Positive flow is to the east.

Latitude limits	Surface layer	EUC core layer	NEUC/SEUC core layer
March 1981			
5°N–6°N	+5.2	+1.6	+8.4
2°N–4°N	−11.0	−2.8	−7.5
2.7°S–0.5°S	+8.5	+9.2	+17.0
7°S–4°S	−11.5	−0.2	−0.7
Total	−8.8	+7.8	+17.2
June 1981			
5.5°N	+5.3	+0.8	+2.6
1.5°N–4.5°N*	−17.7	−2.3	−2.9
2.5°S–0.5°N	+8.7	+11.3	+1.5
3.5°S–5.5°S	−5.7	+0.4	+2.3
6.5°S	+0.9	+0.2	0.0
Total	−8.5	+10.4	+3.5

* Transports at 3.5°N linearly interpolated using stations at 2.5°N and 4.5°N.

The zero-crossing for this mode is about 1200 m. The fact that this eastward velocity increase extended to at least 700 m is consistent with the low-mode nature of the increase.

In June when the flow beneath the Undercurrent is westward, the net transport down to $\sigma_t = 26.5$ surface is to the west at about 5×10^6 m^3 s^{-1} (5 Sv). If transports are examined above a shallower density surface, for example, $\sigma_t = 26.0$, it is obvious that eastward and westward transports occur at different levels. The bulk of the westward transport occurs above the thermocline (above $\sigma_t = 24.9$). The eastward flow is the Undercurrent at a deeper level. The sum of these transports almost cancels, both in March and June. This suggests that the bulk of the Undercurrent might be upwelled into the surface layers between 110°W and the Galápagos and recirculate to the west in the surface layers. The salinity distributions on all three cruises indicate a region of salinities with values greater than 34.9‰ north of the Undercurrent. However, the transports within the σ_t-range of 24.9 to 26.0 suggest that less than 25% of the EUC transport is returning west at these salinities.

REFERENCES

Busalacchi, A. J., and J. J. O'Brien, 1980: The seasonal variability in a model of the tropical Pacific. *J. Phys. Oceanogr.*, **10**, 529–540.

Cromwell, T., 1953: Circulation in a meridional plane in the central equatorial Pacific. *J. Mar. Res.*, **12**, 196–213.

Hayes, S. P., 1982: A comparison of measured and geostrophic velocity in the Equatorial Undercurrent. *J. Mar. Res.*, **40**(Suppl), 219–229.

——, and D. Halpern, 1983: Equatorial waves in eastern Pacific current and sea level measurements. (unpublished manuscript).

——, J. M. Toole and L. J. Mangum, 1983: Water mass and transport variability at 110°W in the equatorial Pacific. *J. Phys. Oceanogr.*, **13**, 153–168.

Leetmaa, A., 1982: Observations of near equatorial flows in the eastern Pacific. *J. Mar. Res.*, **40**, 357–370 (Suppl).

——, and P. F. Spain, 1981: Results from a velocity transect along the equator from 125°W. *J. Phys. Oceanogr.*, **11,** 1030–1083.

——, and D. Wilson, 1983: Characteristics of near surface circulation patterns in the eastern equatorial Pacific. Submitted to *Progress in Oceanography.*

Lucas, R. B., 1982: The termination of the Equatorial Undercurrent in the eastern Pacific. Ph.D. dissertation, University of Hawaii, 127 pp.

Mangum, L. J., N. N. Soreide, B. D. Davies, B. D. Spell and S. P. Hayes, 1980: *CTD/O_2 measurements during the Equatorial Pacific Ocean Climate Study (EPOCS) in 1977.* NOAA Data Rep., ERL-PMEL-1, 621 pp.

Puls, C., 1895: Oberflächentemperaturen und Strömungsverhältnisse des Äquatorialgürtels des Stillen Ozeans. *Aus d. Archiv Dtsch. Seewarte,* **18,** No. 1, 38 pp. & 4 Tafeln.

Robinson, M. K., 1976: *Atlas of North Pacific Ocean Monthly Mean Temperatures and Mean Salinities of the Surface Layer.* Ref. Pub. 2, Naval Oceanographic Office, 173 figures.

Spain, P. F., D. Dorson and H. T. Rossby, 1981: Pegasus: a simple velocity profiler. *Deep-Sea Res.*, **28,** 1553–1567.

Stroup, E. D., 1969: The thermostad of the 13°C water in the equatorial Pacific Ocean. Ph.D. dissertation, Johns Hopkins University, 205 pp.

Sverdrup, H. U., 1947: Wind-driven currents in a baroclinic ocean; with application to the equatorial currents of the eastern Pacific. *Proc. Natl. Acad. Sci. Wash.*, **33,** 308–326.

Taft, B. A., and J. H. Jones, 1973: Measurements of the Equatorial Undercurrent in the eastern Pacific. B. Warren, Ed., *Progress in Oceanography,* **6,** Pergamon, 47–110.

Tsuchiya, M., 1968: Upper waters of the intertropical Pacific Ocean. Johns Hopkins Ocean Study No. 4, Johns Hopkins Press, 50 pp.

——, 1975: Subsurface countercurrents in the Pacific Ocean. *J. Mar. Res.*, **33**(Suppl), 145–175.

——, 1981: The origin of the Pacific equatorial 13°C water. *J. Phys. Oceanogr.*, **11,** 794–812.

Wyrtki, K., 1974: Equatorial currents in the Pacific (1950 to 1970) and their relations to the trade winds. *J. Phys. Oceanogr.*, **4,** 372–380.

——, and G. Meyers, 1976: The trade wind field over the Pacific Ocean, Part I: The mean field and the mean annual variation. Hawaii Institute of Geophysics Rep. No. HIG-75-1, 26 pp.